OXFORD

SOT | Society of Toxicology
academic.oup.com/toxsci

TOXICOLOGICAL SCIENCES, 185(2), 2022, 158–169

https://doi.org/10.1093/toxsci/kfab131
Advance Access Publication Date: 2 November 2021
Research Article

APAP-Induced IκBβ/NFκB Signaling Drives Hepatic Il6 Expression and Associated Sinusoidal Dilation

Laura G. Sherlock,* Durganili Balasubramaniyan,* Lijun Zheng,* Maya Grayck,* William C. McCarthy,* Robert C. De Dios,* Miguel A. Zarate,* David J. Orlicky,† Robyn De Dios,* and Clyde J. Wright*,[1]

*Section of Neonatology, Department of Pediatrics, University of Colorado School of Medicine, Aurora, Colorado, USA, and †Department of Pathology, University of Colorado Anschutz School of Medicine, Aurora, Colorado, USA

[1]To whom correspondence should be addressed at Section of Neonatology, Department of Pediatrics, University of Colorado School of Medicine, Perinatal Research Center, 13243 East 23rd Avenue, Mail Stop F441 Aurora, CO 80045, USA. E-mail: clyde.wright@cuanschutz.edu.

ABSTRACT

Acetaminophen (APAP) overdose results in high morbidity and mortality, with limited treatment options. Increased understanding of the cellular signaling pathways activated in response to toxic APAP exposure is needed to provide insight into novel therapeutic strategies. Toxic APAP exposure induces hepatic nuclear factor kappa B (NFκB) activation. NFκB signaling has been identified to mediate the proinflammatory response but also induces a prosurvival and regenerative response. It is currently unknown whether potentiating NFkB activation would be injurious or advantageous after APAP overdose. The NFκB inhibitory protein beta (IκBβ) dictates the duration and degree of the NFκB response following exposure to oxidative injuries. Thus, we sought to determine whether IκBβ/NFκB signaling contributes to APAP-induced hepatic injury. At late time points (24 h) following toxic APAP exposures, mice expressing only IκBβ knock-in mice (AKBI mice) exhibited increased serologic evidence of hepatic injury. This corresponded with increased histologic injury, specifically related to sinusoidal dilatation. When compared with wild type mice, AKBI mice demonstrated sustained hepatic nuclear translocation of the NFκB subunits p65 and p50, and enhanced NFκB target gene expression. This included increased expression of interleukin-6 (Il-6), a known contributor to hepatic sinusoidal dilation. This transcriptional response corresponded with increased plasma protein content of Il-6, as well as increased activation of signal transducer and activator of transcription 3.

Key words: Il-6; acetaminophen; sinusoidal dilation; IκBβ, NFκB; liver injury; histopathology.

Acetaminophen (N-acetyl-p-aminophenol, APAP) overdose is one of the most common toxic drug exposures, resulting in 40%–70% of the acute liver failure cases in the United States and Europe (Bernal and Wendon, 2013; Bernal *et al.*, 2015). Current treatment strategies are limited to supportive care and N-acetylcysteine, a therapeutic which rapidly loses efficacy when not delivered early after APAP exposure(Yoon *et al.*, 2016). There is an urgent need to investigate the cellular signaling and molecular mechanisms that occur during later phases of injury after APAP, in order to identify alternative treatment strategies.

The sequence of cellular events leading to hepatotoxicity after APAP overdose has been studied by many. Hepatic damage is mediated by increased inflammatory and oxidative stress (Yoon *et al.*, 2016). APAP overdose results in accumulation of the toxic metabolite N-acetyl-p-benzoquinone imine (NAPQI; Yoon *et al.*, 2016). This compound can be inactivated by conjugation with the antioxidant glutathione (GSH; Yoon *et al.*, 2016). However, excess NAPQI binds cellular proteins, inducing mitochondrial dysfunction and resulting in increased oxidative stress (Yoon *et al.*, 2016). Toxic APAP doses also can deplete hepatic antioxidant enzymes (AOEs) and antioxidants including

© The Author(s) 2021. Published by Oxford University Press on behalf of the Society of Toxicology. All rights reserved.
For permissions, please e-mail: journals.permissions@oup.com

GSH, exacerbating oxidative stress (Yan *et al.*, 2018). This oxidative stress activates redox sensitive signaling pathways, perpetuating the inflammatory response and inducing necrosis and cell death (Yan *et al.*, 2018). One proinflammatory pathway that is activated after APAP is the nuclear factor kappa B (NFκB) signaling pathway (Yan *et al.*, 2018).

Evidence is clear that hepatic NFκB activation occurs after toxic APAP exposure (Chowdhury *et al.*, 2020; Ding *et al.*, 2016; Ko *et al.*, 2017; Long *et al.*, 2020). Active NFκB signaling increases the transcription for a myriad of inflammatory cytokines and chemokines, as well as proteins that regulate cell survival and apoptosis (Hayden and Ghosh, 2008; Zhang *et al.*, 2017). It has been demonstrated that several interventions that attenuate hepatic injury after toxic APAP exposure are associated with decreased NFκB activation and downstream cytokine generation (Ding *et al.*, 2016; Horng *et al.*, 2017; Ko *et al.*, 2017; Long *et al.*, 2020; Yuan *et al.*, 2016). However, NFκB activation after APAP exposure is not always detrimental, as it is important for signaling liver regenerative pathways (Chowdhury *et al.*, 2020; Yang *et al.*, 2011, 2012). Thus, it is currently unclear if potentiating NFκB activation after APAP exposure would be injurious or beneficial.

To clarify, the nuanced role of NFκB activation after APAP exposure requires evaluation of the specific components of the NFκB signaling cascade. Under control conditions, NFkB subunits are cloistered in the cytoplasm by the inhibitory proteins, IkappaB alpha (IκBα), and IkappaB beta (IκBβ). After exposure to damage-associated molecular patterns and pathogen-associated molecular patterns, activity of the IκB kinases increases, which phosphorylate IκBα and IκBβ (Taniguchi and Karin, 2018; Zhang *et al.*, 2017), targeting them for degradation. Following degradation of these inhibitory proteins, NFκB dimers translocate to the nucleus and drive transcription. Each NFκB inhibitory protein selectively regulates NFkB dimer composition and subsequent gene expression (Hayden and Ghosh, 2008). Enhancing or blocking these specific NFκB components after APAP exposure could provide insight into the molecular mechanisms of APAP-induced hepatoxicity; however, such investigations have been relatively limited.

The specific role of IκBβ in mediating APAP-induced hepatotoxicity warrants investigation, as it has both the cytoplasmic inhibitory role described above, as well as a nuclear role in sustaining expression of a subset of NFκB target genes following activation (Rao *et al.*, 2010; Scheibel *et al.*, 2010). With reaccumulation following cytosolic degradation, both IκBα and IκBβ enter the nucleus. The NFκB inhibitory protein α (IκBα) contains a nuclear export sequence and acts to remove transcriptionally active NFκB dimers from the nucleus (Huang *et al.*, 2000). In contrast, IκBβ does not contain a nuclear export sequence, and acts to stabilize active DNA-bound NFκB dimers, increasing transcription of a subset of NFκB target genes, including interleukin-6 (Il-6; Scheibel *et al.*, 2010). We have previously shown that mice expressing only IκBβ and no IκBα demonstrate sustained NFκB activation in response to oxidative stress, resulting in increased expression of specific target genes including Il-6 (McKenna *et al.*, 2014; Michaelis *et al.*, 2014). Therefore, we sought to determine the role of IκBβ/NFκB signaling in the hepatic response to toxic APAP exposure.

MATERIALS AND METHODS

Murine model of toxic APAP exposure

Adult (6–8 week old) male Institute of Cancer Research mouse strain (ICR) mice (purchased from Tacoma) were used for wild type (WT) mice with normal expression of both the IκBα and IκBβ genes. IκBβ knock-in mice (AKBI mice) (generous gift from Richard Cohen, Harvard University) were also used. These IκBβ knock-in mice have been previously described (Cheng *et al.*, 1998). Briefly, the IκBα gene is replaced by IκBβ complementary deoxyribonucleic acid (cDNA). Thus, AKBI mice overexpress IκBβ and do not express the inhibitory protein IκBα at baseline. Mice were fasted overnight prior to exposure. ICR and AKBI were exposed to APAP at a dose of 280 mg/kg, delivered intraperitoneally (IP); dissolved in phosphate-buffered saline. Mice were sacrificed, and blood and organs were collected 8 and 24 h after exposure. The blood was collected by a cardiac puncture through a closed chest. Then, 10 ml of normal saline was injected into the right ventricle to perfuse the lungs. Liver samples were collected and processed for biochemical, transcriptomic, and histologic analysis all as described below. All procedures were approved by the IACUC at the University of Colorado (Aurora, Colorado). Treatment, care, and handling of the mice were in accordance with the National Institutes of Health guidelines for ethical animal treatment.

Serum alanine aminotransferase and high mobility group B1 measurements

Serum alanine aminotransferase (ALT) was quantitatively determined by using a colorimetric endpoint method according to the manufacturer's instructions, using an ALT (SGPT) reagent (Teco Diagnostics). Serum high mobility group B1 (HMGB1) was measured by ELISA following the accompanying protocol (MyBiosource).

Histologic evaluation of APAP-induced hepatic injury

A section of liver was processed by fixing with 4% paraformaldehyde, then paraffin-embedded. Hepatic sections were cut (5 μm) and stained with hematoxylin and eosin at the University of Colorado Denver Morphology and Phenotyping Core. Histopathological scoring of the liver tissue was performed by a trained histologist blinded to the treatments or grouping of animals, as previously described (Martin-Murphy *et al.*, 2013; Sandoval *et al.*, 2019). Briefly, the APAP-induced liver injury system used relied on 3 semiquantitative and 1 quantitative criteria. These criteria including: (1) extent and locale of necrosis (0–5 scale: how big the necrotic foci are, where they are found, does the necrosis occupy the whole lobule?), (2) the extent of inflammatory cell infiltrate (0–5 scale: how many cells are observed and in which zone are they present), (3) the extent of centrilobular sinusoidal dilatation (0–2 scale: how wide are the centrilobular sinusoids in comparison to the width of a murine red blood cell), and (4) measurement of the serum ALT all as indicated in Martin-Murphy *et al.* (2013) A full description of the scoring is listed in Table 1.

Hepatic GSH fluorescent detection

Whole liver tissue was homogenized. Hepatic lysates were collected in tissue protein extraction reagent (T-PER) (ThermoFisher Scientific). GSH contents were quantified using the GSH fluorescent detection kit according to manufacturer instructions (ThermoFisher Scientific).

GSH peroxidase activity level

The activity level of GSH peroxidase (GPx) was determined indirectly by a coupled reaction with GSH reductase, as previously described (Sherlock *et al.*, 2020). Briefly, 20 mg of liver was lysed

Table 1. Description of Histolopathological Scoring Criteria, as Previously Published By Martin-Murphy *et al.* (2013)

1. Histopathological evaluation for *necrosis* included, but was not limited to, assessing the distribution and extent of cell death (hepatocytes and nonparenchymal cells). Lesions were graded on a semiquantitative scale:
   0, Normal
   1, Rare foci of necrotic cells in centrilobular zones (no more than 1–2 sites per section)
   2, Few necrotic foci (less than half of centrilobular zones had sites of necrosis)
   3, Many/diffuse centrilobular zones with necrosis (confined to centrilobular zone only)
   4, Diffuse centrilobular to midzonal necrosis
   5, Diffuse submassive to massive necrosis (most or almost all of lobule was necrotic)
2. The extent of *inflammatory cellular infiltration* into the liver was examined using the same liver samples as for histopathology. Cellular infiltration was graded visually on a semiquantitative scale:
   0, No influx
   1, Rare inflammatory cells (no more than 1–3 cells in 1 or 2 centrilobular zones per section)
   2, Few inflammatory cells (1–5 cells in <50% of centrilobular zones)
   3, Moderate inflammatory cell infiltration (5–15 cells in most centrilobular zones)
   4, Marked inflammatory cell infiltration (>15 cells in most centrilobular to midzonal areas)
   5, Severe inflammatory cell infiltration (too numerous to count and infiltrating most of lobule)

Note: In all cases where inflammation is noted, please identify the cell type

3. *Sinusoidal dilation* on a semiquantitative scale:
   0, Normal or approximately 1 RBC wide
   1, Dilated to 2–3 RBCs wide, mainly in the centri-lobular area (zone 3)
   2, Grossly dilated or beyond 3 RBCs in diameter in zones 3 and 2

in buffer with 1 mM sodium azide to block endogenous catalase activity. This was added to a reaction buffer with GSH reductase, reduced GSH, and NADPH. Hydrogen peroxide was used to catalyze the reaction, which was then monitored at 340 nm on a microplate reader. GPx activity was calculated using Lambert-Beer's law and activity was normalized to WT control values.

Thioredoxin reductase activity level

The activity level of thioredoxin reductase (Trxrd) was determined indirectly by a coupled reaction with NADPH and 5, 5- dithio-bis-(2-nitrobenzoic acid), as previously described and using manufacturer instructions (Cayman Chemicals). Activity was normalized to WT control values.

Isolation of mRNA, cDNA synthesis, and analysis of relative mRNA levels by real-time quantitative PCR

Frozen liver was added to tubes with RLT buffer (Qiagen). This was then homogenized using the Bullet Blender (NextAdvance). Hepatic messenger ribonucleic acid (mRNA) was subsequently isolated from this by using the RNeasy Mini Kit (Qiagen) according to the manufacturer's instructions. Hepatic RNA was assessed for purity and concentration using a NanoDrop (ThermoFisher Scientific). Next, cDNA was synthesized using the Verso cDNA synthesis Kit (ThermoFisher Scientific). Then, relative mRNA levels were measured by quantitative real-time PCR using exon spanning primers (Table 2), TaqMan gene expression, and StepOnePlus Real-Time PCR System (Applied Biosystems). Relative quantitation was determined via normalization to the endogenous control 18S using the cycle threshold ($\Delta\Delta C_t$) method.

Preparation of whole liver lysate and cytosolic/nuclear extracts and Western blot

Frozen liver was added to T-PER with phosphatase and protease inhibitor (1:100) and then homogenized using the Bullet Blender (NextAdvance). Cytosolic and nuclear extracts were electrophoresed on a 4%–12% polyacrylamide gel (Invitrogen). Proteins were transferred to an Immobilon membrane (Millipore) and blotted with antibodies (Table 3). Blots were imaged using the LiCor Odyssey imaging system and densitometric analysis was performed using ImageStudio (LiCor).

Statistical analysis

We used the null hypothesis that no difference existed between treatments. We evaluated data using 1-way ANOVA for multiple groups with potentially interacting variables (time, APAP exposure). All groups contained at least 4 animals. Statistical significance between and within groups determined by means of Dunnett's method of multiple comparisons. To compare similar time points after exposure between genotypes, student's t tests were used. Statistics were evaluated using Prism (GraphPad Software, Inc). Statistical significance was defined as $p < .05$.

RESULTS

Baseline Expression of Hepatic NFκB Inhibitory Proteins is Different in AKBI Mice. Hepatic Expression of APAP Metabolizing Enzyme CYP2E1 is Similarly Expressed to WT Mice

First, we measured the hepatic protein content of the NFκB inhibitory proteins, IκBα and IκBβ. As expected, in comparison to WT mice, AKBI mice have undetectable IκBα protein content and twice the IκBβ protein content (Figs. 1A–C). Prior reports illustrate these mice are phenotypically similar to WT mice, with similar lifespans and fertility. However, we sought to determine if there was any difference in expression of key xenobiotic enzymes important for metabolizing APAP between genotypes. Thus, we next evaluated if there was any baseline difference in CYP2E1 hepatic transcription or protein content in the liver of unexposed WT and AKBI mice. There was no difference in the mRNA (Figure 1D) or protein content (Figs. 1A and 1E).

AKBI Mice Demonstrate a Delayed but Exaggerated Biochemical Injury After APAP

Next, we assessed circulating markers of liver injury in WT and AKBI mice following a single toxic APAP exposure (280 mg/kg, IP). Circulating ALT increased in WT mice at both 8 and 24 h after

Table 2. List of Genes and Primers Used for Quantitative PCR Analysis

Target	Assay ID
Nqo1	Mm01253561_m1
Gclc	Mm00802655_m1
Trxrd1	Mm0049766_m1
Nos2	Mm00440502_m1
Il1b	Mm01336189_m1
Tnf	Mm00443258_m1
Cxcl1	Mm04207460_m1
Ccl2	Mm00441242_m1
Ccl3	Mm99999057_m1
Icam	Mm00516023
Il6	Mm00446190_m1
18s	Mm03928990_g1

Table 3. List of Antibodies Used for Western Blot Analysis

Antibody	Vendor	Catalog Number
Anti-GAPDH	Cell Signaling Technology	5174
Anti-IκBβ	Thermofisher Invitrogen	PA1-32136
Anti- IκBα	Cell Signaling Technology	4814
Anti-p65	Cell Signaling Technology	8242
Anti-p50	Abcam	ab32360
Anti-HDAC1	Cell Signaling Technology	5356
Anti-P-stat3	Cell Signaling Technology	9145
Anti-Stat3	Cell Signaling Technology	12 640

Abbreviation: GAP DH, glyceraldehyde 3-phosphate.

APAP exposure (Figure 2A). We found that the rise in serum ALT was lower in AKBI mice compared with WT mice at 8 h. In contrast, at 24 h following APAP exposure, circulating ALT values were significantly higher in AKBI mice, with a percentage increase of 103% compared with WT values at this time (Figure 2A). Similarly, the rise in HMGB1 was lower in AKBI compared with WT mice at 8 h, but significantly higher at 24 h after injury (increase of 273% compared with WT values) (Figure 2B). These results demonstrate that following toxic APAP exposure, AKBI mice demonstrated a delayed but exacerbated rise in serologic markers of hepatic injury when compared with similarly exposed WT mice.

AKBI Mice Exhibit Worse Hepatic Necrosis Than WT Mice After Toxic APAP Exposure

Next, we performed histologic evaluation for necrosis and inflammatory injury in the liver after toxic APAP exposure in both WT and AKBI mice. Blinded histopathologic analysis revealed that necrosis (Figure 3E), inflammatory infiltration (Figure 3F), and sinusoidal dilation (Figure 3G) increased in both WT and AKBI mice livers at 8 and 24 h after APAP exposure. However, the AKBI mice exhibited higher hepatic necrosis and sinusoidal dilation scores than WT mice at 24 h (Figs. 3E and 3G). These results demonstrate that at later time points following toxic APAP exposure, AKBI mice have increased hepatic necrosis and sinusoidal dilation compared with similarly exposed WT mice.

AKBI Mice Have Increased Hepatic Transcription for Oxidative Stress Responsive Genes

Oxidative stress contributes to APAP-induced hepatic injury (Yan *et al.*, 2018). Prior work demonstrates APAP impairs hepatic AOEs including GPx and Trxrd, as well as depletes total hepatic GSH (Jan *et al.*, 2014; Lores Arnaiz *et al.*, 1995). Thus, we interrogated antioxidant activity and AOE expression at 24 h of exposure when AKBI hepatic injury was greatest. Interestingly, we observed that control AKBI mice had 13% lower hepatic GSH levels than WT mice at baseline (Figure 4A). However, we found that the total decrease in hepatic GSH observed at 24 h after APAP exposure was similar in WT and AKBI mice (Figure 4A). After observing a decrease in hepatic GSH at baseline between strains, we subsequently evaluated if there was a difference in the transcription of the enzymes required for GSH biosynthesis, glutamate-cysteine ligase catalytic subunit (*Gclc*), and glutamate-cysteine ligase modifier subunit (*Gclm*). The mRNA expression of Gclc (Figure 4B) and Gclm (Figure 4C) was similar in unexposed control WT and AKBI mice. We next evaluated the AOE activity levels of GPx and Trxrd, as they have been reported to decrease at early time points after toxic APAP doses(Jan *et al.*, 2014; Lores Arnaiz *et al.*, 1995). Hepatic GPx activity decreased in both WT and AKBI mice 24 h after APAP exposure (Figure 4B); however, activity was significantly lower in AKBI mice than WT (Figure 4D). In contrast, hepatic Trxrd activity was similar to control levels in both WT and AKBI mice 24 h after APAP exposure (Figure 4E). Next, we measured the transcriptional response in oxidative stress-responsive genes after APAP. We found *Nqo1* increased in both WT and AKBI mice at both 8 and 24 h, but the increase in AKBI mice was significantly greater than that of the WT mice at 24 h, being 168% higher (Figure 4D). Furthermore, we found *Gclc* and *Trxrd1* both increased in WT and AKBI mice at 8 h (Figs. 4E and 4F). At 24 h after APAP exposure, *Gclc* and *Trxrd1* were statistically similar to WT control mice, but remained increased in AKBI mice (Figs. 4E and 4F). These data demonstrate that the AKBI hepatic antioxidant system continues to be affected by toxic APAP exposure extending to these late time points.

AKBI Mice Demonstrate Sustained Hepatic Nuclear Translocation of NFκB Subunits After APAP Exposure

We next evaluated APAP-induced hepatic NFκB signaling in both WT and AKBI mice, focusing on these later time points. We compared NFκB activation within each genotype. In WT mice, there was no evidence of hepatic IκBα or IκBβ degradation at 8 or 24 h after APAP exposure (Figs. 5A–C). AKBI mice were confirmed to not express hepatic IκBα under control conditions or after APAP (Figs. 5A and 5B). In AKBI mice, we observed hepatic IκBβ degradation at 24 h after APAP exposure (Figs. 5A and 5C). Next, we evaluated hepatic nuclear extracts for the translocation of the NFκB subunits p50 and p65. In WT mice, there was no evidence of nuclear translocation of p50 or p65 at either 8 or 24 h of exposure (Figs. 5D–F). In contrast, we found increased p50 and p65 in hepatic nuclear extracts from AKBI mice following 24 h of APAP exposure (Figs. 5D–F).

AKBI Mice Exhibit a Delayed but Exaggerated Hepatic Transcriptional Induction of NFκB Target Genes

After observing increased nuclear translocation of p50 and p65 after 24 h of APAP exposure in AKBI mice, we evaluated the hepatic transcriptional response for NFκB target genes. First, we found that *Nos2* did not significantly increase in WT mice at 8 or 24 h but did statistically increase in AKBI mice at 24 h (Figure 6A). Additionally, *Il-1B* was increased in both WT and AKBI mice at 8 and 24 h but had 276% higher values in AKBI mice compared with WT mice at 24 h (Figure 6B). *Tnf* was increased in WT mice

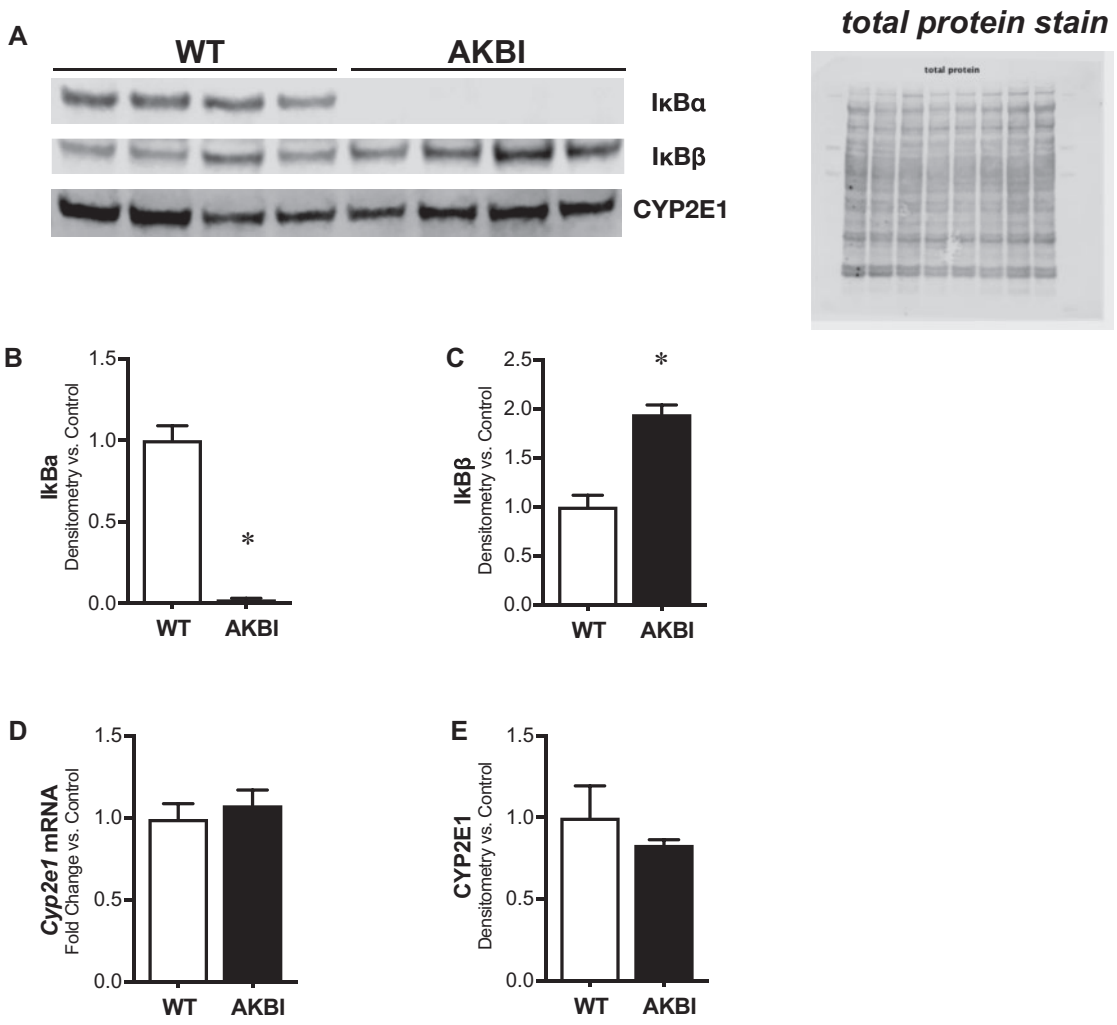

Figure 1. Time course of serologic evidence of acetaminophen-induced hepatic injury in wild type (WT) and AKBI mice. WT and AKBI (IkappaB beta [IκBβ] knock-in mice) unexposed mice were evaluated. A, Representative Western blot of nuclear factor kappa B inhibitory proteins IkappaB alpha (IκBα) and IκBβ, as well as CYP2E1, in hepatic lysates, with total protein shown as loading control. Densitometric analysis of B, IκBα and C, IκBβ in hepatic lysates. D, Fold change hepatic mRNA expression of *Cyp2e1*. E, Densitometric analysis of CYP2E1 in hepatic lysates. White columns represent WT mice and black columns represent AKBI mice ($n = 4$–8). Data are expressed as mean ± SEM; *$p < .05$ versus unexposed WT-controls.

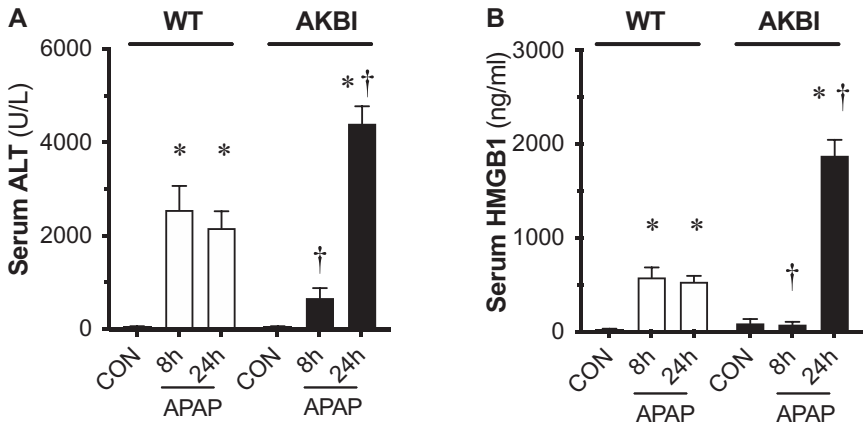

Figure 2. Time course of serologic evidence of acetaminophen (APAP)-induced hepatic injury in wild type (WT) and AKBI mice. WT and AKBI (IkappaB beta knock-in mice) were exposed to APAP (280 mg/kg, IP) for 0, 8, or 24 h. A, Total serum alanine aminotransferase and B, serum high mobility group B1 protein. White columns represent WT mice and black columns represent AKBI mice ($n = 25$–33). Data are expressed as mean ± SEM; *$p < .05$ versus unexposed genotype-matched control; †$p < .05$ versus similarly time-matched APAP-exposed WT.

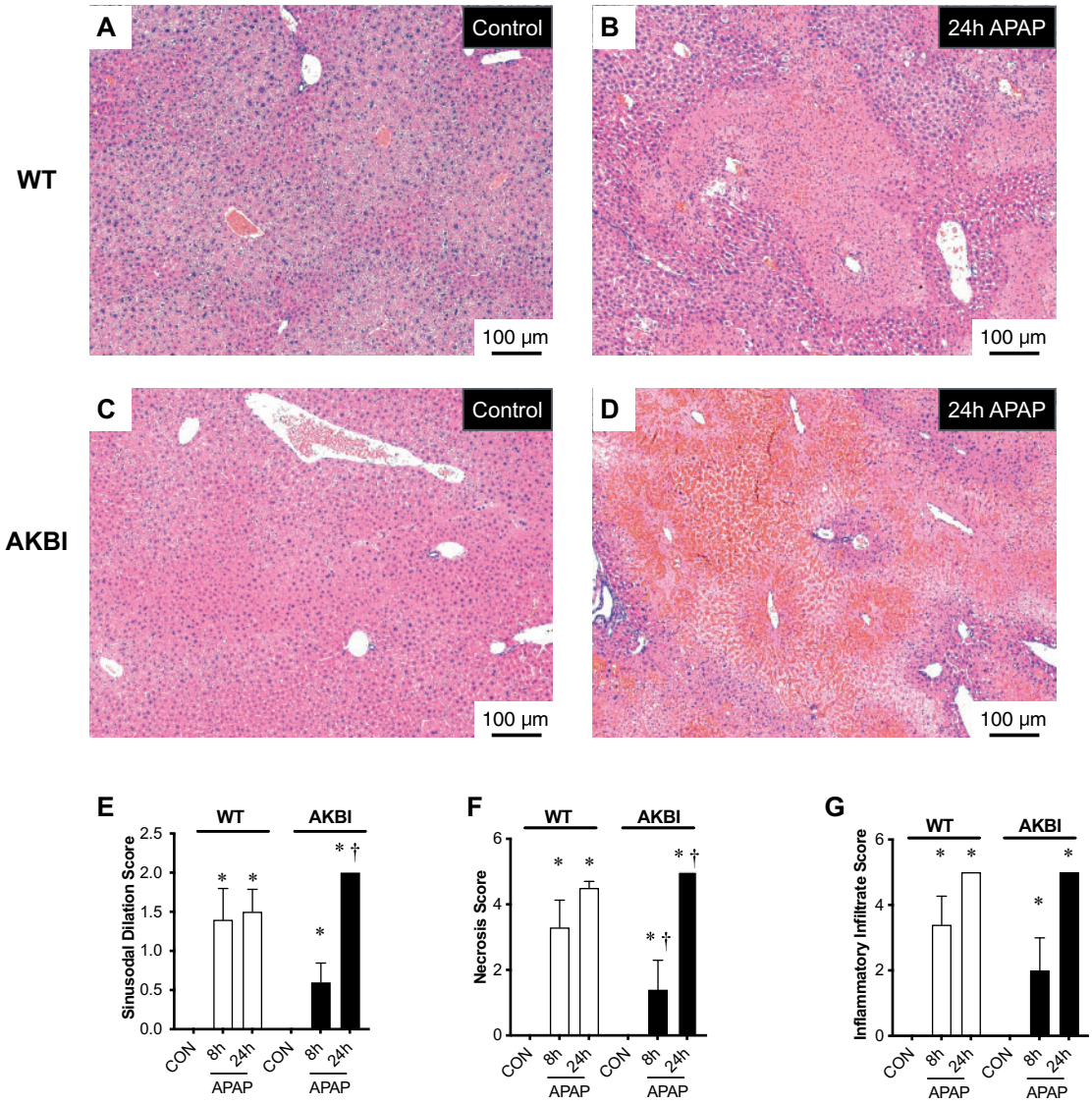

Figure 3. Time course of acetaminophen (APAP)-induced hepatic injury in wild type (WT) and AKBI mice. WT and AKBI (IkappaB beta knock-in mice) were exposed to APAP (280 mg/kg, IP) for 0 or 24 h. A–D, Representative hematoxylin and eosin (H&E)-stained hepatic sections from WT (A and B) and AKBI (C and D) control and APAP exposed (24 h). Internal scale bar 100 μm. E–G, Blind histopathologic evaluation of H&E-stained hepatic sections scored for E, necrosis, F, inflammatory infiltration, and G, sinusoidal dilatation. White columns represent WT mice and black columns represent AKBI mice ($n = 4$–6). Data are expressed as mean ± SEM; *$p < .05$ versus unexposed genotype-matched control; †$p < .05$ versus similarly time-matched APAP-exposed WT.

at 8 and 24 h but only increased in AKBI mice at 24 h (Figure 6C). *Tnf* values were 174% higher in AKBI mice compared with WT mice at 24 h, although the increase at 24 h was not statistically different between WT and AKBI mice ($p = .051$). *Cxcl1*, *Ccl2*, and *Ccl3* were increased in WT mice at 8 and 24 h and were only increased in AKBI mice at 24 h (Figs. 6D–F). The increase in AKBI mice at 24 h was significantly greater than the increase in WT mice, by 326% for *Cxcl1*, 276% for *Ccl2*, and 193% by *Ccl3*. Next, we measured the adhesion molecule *Icam1*, and found it only increased in WT mice at 24 h after APAP (Figure 6G). In contrast, it increased at 8 and 24 h after APAP in AKBI mice and AKBI *Icam1* values were 135% higher than WT mice at 8 h (Figure 6G). Finally, we measured *Il-6* and found it was increased in WT mice at 8 h and remained increased but trending down at 24 h. In contrast, *Il-6* was only increased in AKBI mice at 24 h and was 260% higher than WT values at this time (Figure 6H). These data indicate a greater induction of NFκB target genes in AKBI mice 24 h after APAP injury.

AKBI Mice Exhibit Increased Circulating Il-6 and Hepatic Signal Transducer and Activator of Transcription 3 Activation

Prior preclinical and clinical work demonstrates that high plasma Il-6 is associated with severe APAP injury (Bonkovsky *et al.*, 2018; Bourdi *et al.*, 2007; James *et al.*, 2005). Additionally, Il-6 and the signaling pathways that it activates are reported to drive drug-induced and systemic inflammatory-induced hepatic sinusoidal dilation, which was prominent in the AKBI mice (Marzano *et al.*, 2015; Robinson *et al.*, 2013). Thus, we next sought to explore if the increase in hepatic *Il-6* transcription was associated with an increased circulating Il-6 or signal transducer and activator of transcription 3 (STAT3) activation, which is a pathway activated by Il-

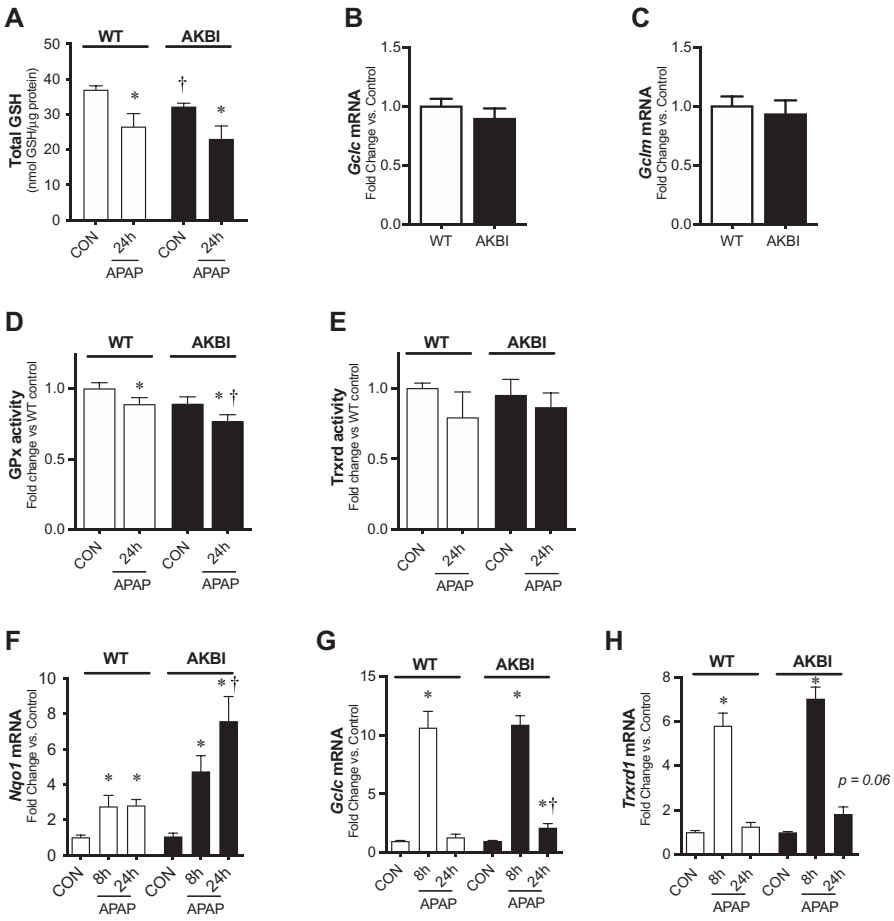

Figure 4. Hepatic redox response to acetaminophen (APAP) exposure (280 mg/kg, IP) in wild type (WT) and AKBI mice. WT and AKBI (IkappaB beta knock-in mice) were exposed to APAP (280 mg/kg, IP) for 0, 8, or 24 h. A, Total glutathione protein content. Fold change hepatic mRNA expression of B, *Gclc*, C, *Gclm* in unexposed mice. D, Glutathione peroxidase activity, expressed as fold change from WT control. E, Thioredoxin reductase (Trxrd) activity, expressed as fold change from WT control. Fold change hepatic mRNA expression of F, *Nqo1*, G, *Gclc*, H, *Trxrd1*. White columns represent WT mice and black columns represent AKBI mice ($n = 4$–20). Data are expressed as mean ± SEM; *$p < .05$ versus genotype-matched control and †$p < .05$ versus time-matched exposure.

6. Because our data demonstrated hepatic Il-6 transcription was increased in AKBI mice by 24 h, we focused our assessment at this timepoint. As Il-6 is secreted into the circulation, we first measured plasma Il-6 and found it was increased in both WT and AKBI mice 24 h after APAP exposure (Figure 7A). However, the increase was significantly higher in AKBI mice, with an increase of 130% compared with WT values. Next, we measured hepatic phosphorylated STAT3 (pSTAT3) and total STAT3. Hepatic pSTAT3 and STAT3 content increased in both WT and AKBI mice after APAP exposure (Figs. 7B–D). The ratio of pSTAT3/STAT3 was only significantly elevated in AKBI mice (Figs. 7B and 7E). These data indicate that there is a greater induction of Il-6 as well as hepatic STAT3 activation in AKBI mice after APAP.

DISCUSSION

APAP overdose remains common and there are limited treatment options. Investigation of the hepatic signaling pathways that are activated after APAP exposure is urgently needed to identify future therapeutic agents. We sought to determine the role of the NFκB inhibitory proteins IκBβ and IκBα in the hepatic response to toxic APAP exposure. We found that sustained IκBβ/NFκB signaling exaggerated biochemical injury after toxic APAP exposure, with an increase in serologic markers for hepatic injury 24 h after exposure. Consistently, this was paralleled by worse histopathologic markers of hepatic injury, including necrosis and sinusoidal dilatation. AKBI mice demonstrated sustained APAP-induced hepatic IκBβ/NFκB signaling with a robust hepatic transcriptional response in NFκB target genes Importantly, this included increased expression of Il-6 at late time points. Finally, AKBI exhibited increased hepatic STAT3 signaling at late time points, with an increased phosphorylated STAT3/total STAT3 ratio. Collectively, these findings indicate that sustained NFκB activity mediated by IκBβ contributes to APAP-induced injury.

Our first important observation is that IκBβ knock-in mice demonstrated worse serologic and histologic injury at late time points after exposure to a single toxic APAP exposure. This coincided with an elevated and sustained expression of hepatic cytokine and oxidative stress-responsive genes at late time points after APAP exposure in comparison to WT mice. These findings indicate that sustained IκBβ/NFκB can contribute to APAP-induced hepatotoxicity. Our results are consistent with the observation that increased NFκB activation and associated proinflammatory response is associated with greater hepatotoxicity after APAP exposure (Jiang *et al.*, 2017; Yang *et al.*, 2012). Furthermore, several therapeutic strategies that result in decreased NFκB signaling are associated with attenuated serologic and histologic damage after APAP (Ding *et al.*, 2016; Horng *et al.*, 2017; Ko *et al.*, 2017; Long *et al.*, 2020; Yuan *et al.*, 2016). In

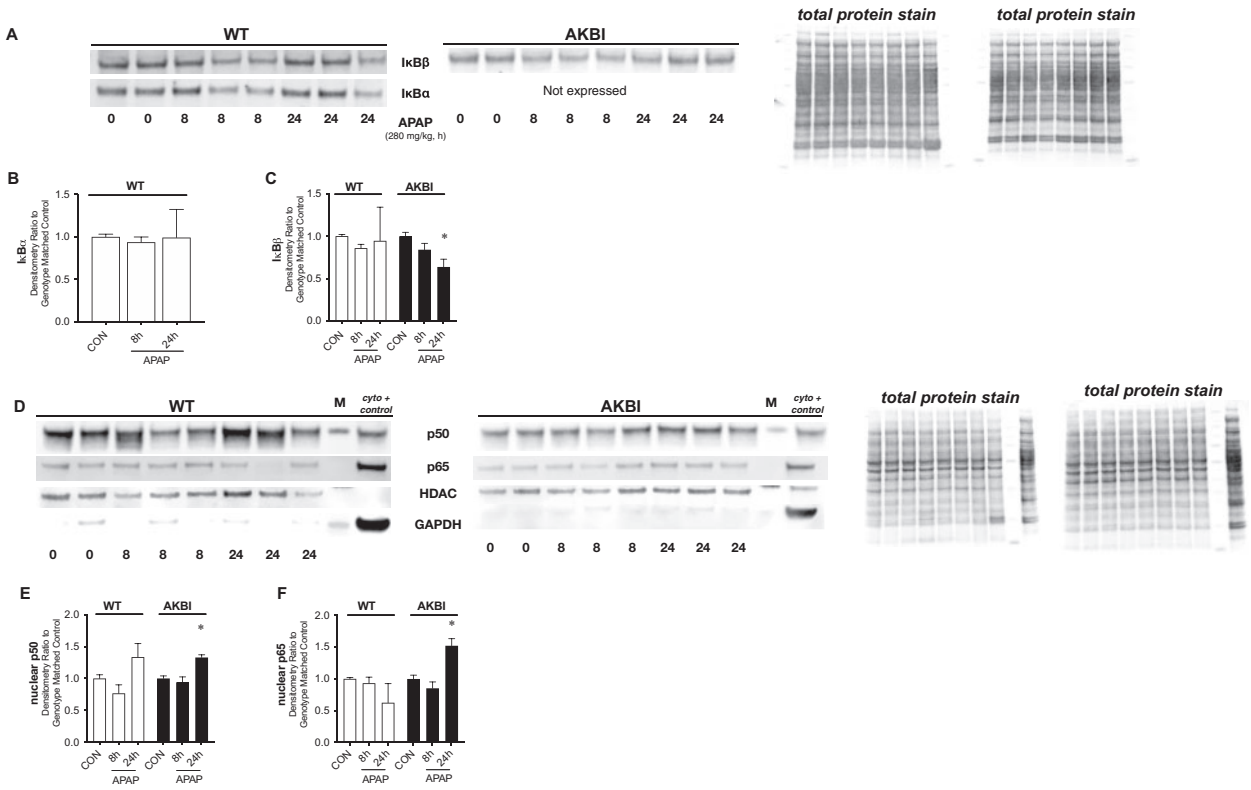

Figure 5. Toxic acetaminophen (APAP) exposure induces sustained hepatic nuclear factor kappa B (NFκB) signaling in AKBI mice. Wild type (WT) and AKBI (IkappaB beta [IκBβ] knock-in mice) were exposed to APAP (280 mg/kg, IP) for 0, 8, or 24 h. A, Representative Western blot of NFκB inhibitory proteins IkappaB alpha (IκBα) and IκBβ in hepatic lysates, with total protein shown as loading control. Densitometric analysis of B, IκBα and C, IκBβ in hepatic lysates after APAP exposure (8 and 24 h; 280 mg/kg, IP). D, Representative Western blot of NFκB subunits p50 and p65 in hepatic nuclear extracts, with total protein shown as loading control. Densitometric analysis of E, p50 and F, p65. White columns represent WT mice and black columns represent AKBI mice ($n = 5$–11). Data are expressed as mean ± SEM; $^*p < .05$ versus genotype-matched control and $\dagger p < .05$ versus time-matched exposure.

addition, our results add to growing evidence that IκBβ enhances the proinflammatory response after certain stimuli. Specifically, IκBβ knock-out mice demonstrate lower circulating cytokines after endotoxemia as well as collagen-induced arthritis (Rao *et al.*, 2010). This is further supported by *in vitro* experiments with IκBβ knock-out peritoneal macrophages and bone marrow-derived macrophages, which demonstrated decreased cytokine response after LPS (Rao *et al.*, 2010). Our findings implicate IκBβ as an important driver of the late phase proinflammatory response following APAP exposure.

We also found IκBβ overexpression resulted in decreased hepatic GSH at baseline. We found this was not a result of decreased transcription of *Gclc* or *Gclm*, 2 of the essential enzymes for GSH synthesis. Hepatic GSH stores are important for conjugating to and inactivating the toxic metabolite NAPQI (Yoon *et al.*, 2016). Prior studies indicate GSH overexpression is protective and GSH depletion exacerbates injury induced by APAP exposure (Botta *et al.*, 2008; McConnachie *et al.*, 2007; Pu *et al.*, 2019). However, in this study, the basal decrease in hepatic GSH for AKBI mice was modest (13%), and the decline after APAP exposure was not exaggerated in AKBI mice, so it cannot be concluded that this limited difference drives the exaggerated injury after APAP. We did observe an increase in several oxidative stress-responsive genes, including *Nqo1*, *Gclc*, and *Trxrd1* in the livers of AKBI mice compared with WT mice, which supports the conclusion that AKBI mice exhibit increased oxidative stress after APAP. The prior research demonstrating the interplay between NFκB activation and oxidative stress is strong (Morgan and Liu, 2011; Nathan and Cunningham-Bussel, 2013). Several NFκB targets are prooxidant, such as *Nos2*, which may contribute to increased generation of free radicals after insult (Morgan and Liu, 2011; Nathan and Cunningham-Bussel, 2013). Additionally, the AKBI liver exhibited decreased activity of the AOE GPx after APAP, which we speculate may hinder the capacity to detoxify reactive oxygen species. Future work will need to investigate the cellular and compartmental source of oxidative stress in mice with IκBβ overexpression after APAP.

This work emphasizes that the precise role of IκBβ in mediating the cellular response to injurious stimuli is nuanced. Despite the worse outcomes at late time points after APAP, the IκBβ knock-in mice demonstrated attenuated serologic and histologic markers of injury at an earlier time point (8 h) after APAP exposure. This is consistent with several publications that demonstrated a protective benefit in IκBβ knock-in mice. It has been reported that IκBβ overexpressing mice exhibit decreased organ injury after hyperoxia-induced lung injury and angiotensin-2-induced hypertension and myocardial injury (McKenna *et al.*, 2014; Michaelis *et al.*, 2014; Xu *et al.*, 2011). Prior work also reveals that the protection secondary to IκBβ overexpression can be hepatic specific, as AKBI mice exhibit improved survival and decreased hepatic inflammatory cytokine production after endotoxin-induced shock and hepatic ischemia/reperfusion injury (Fan *et al.*, 2004; McKenna *et al.*, 2015). Collectively, our work adds to prior studies indicating that the IκB isoforms play specific roles in determining whether NFκB signaling is protective or deleterious, and depends on the time point,

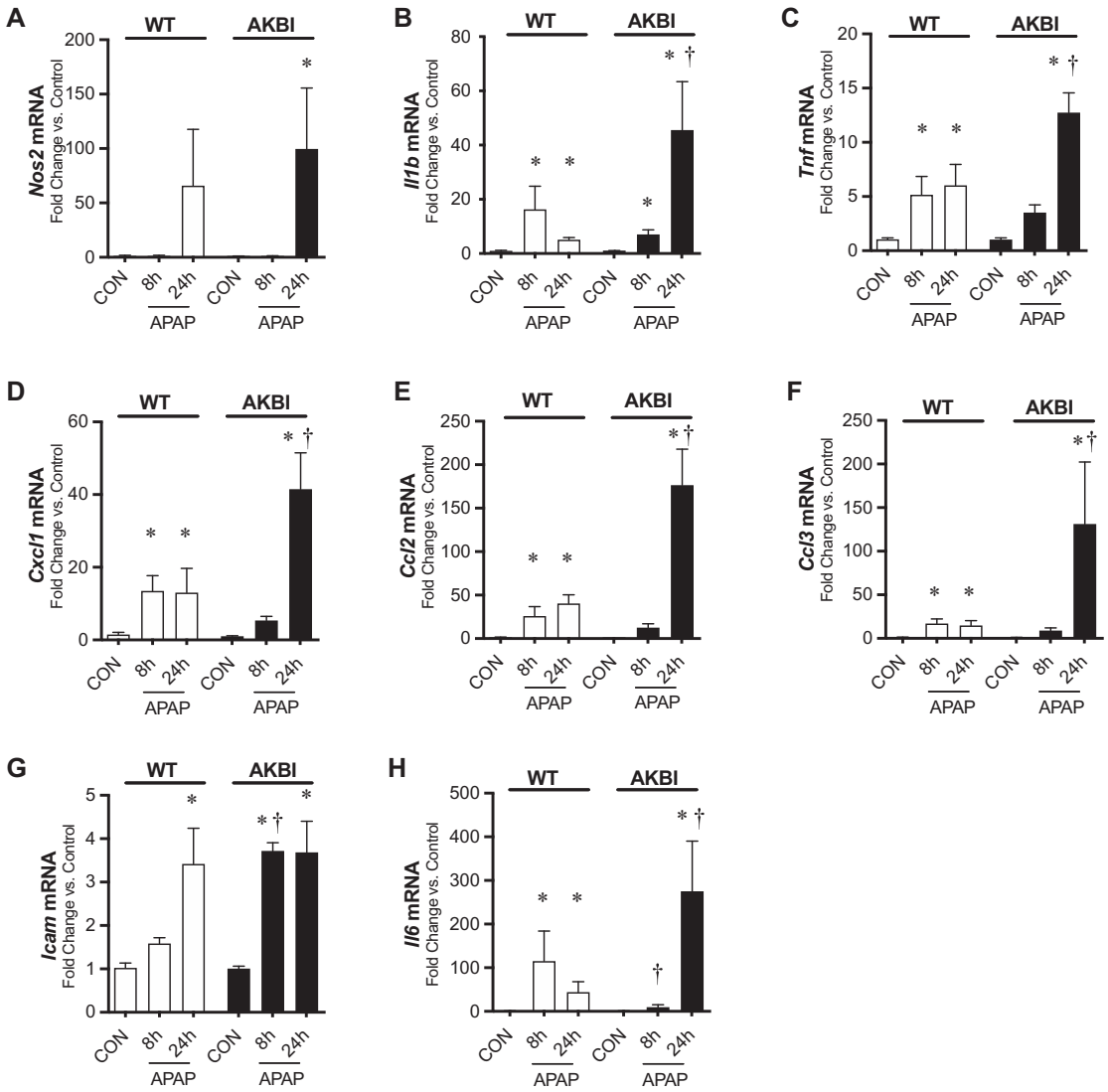

Figure 6. Hepatic nuclear factor kappa B (NFκB) transcriptional response to acetaminophen (APAP) exposure in wild type (WT) and AKBI mice. WT and AKBI (IkappaB beta knock-in mice) were exposed to APAP (280 mg/kg, IP) for 0, 8, or 24 h. Fold change hepatic mRNA expression of A, *Nos2*, B, *Il1b*, C, *Tnf*, D, *Cxcl1*, E, *Ccl2*, F, *Ccl3*, G, *Icam1*, and H, *Il6*. White columns represent WT mice and black columns represent AKBI mice ($n = 5$–21). Data are expressed as mean ± SEM; *$p < .05$ versus genotype-matched control and †$p < .05$ versus time-matched exposure.

specific insult, and organ considered. It is unclear in this study if the delayed increase in biochemical, histological, and hepatic inflammatory cytokines after APAP exposure in the AKBI mice is secondary to the absence of IkBα or the overexpression of IκBβ. Future work will need to clarify the nuanced roles of the abundance and ratio of NFκB inhibitory proteins after insult.

Our next important observation is that mice exclusively expressing the inhibitory protein IκBβ demonstrated increased hepatic transcription of several inflammatory cytokines including Il-6 at 24 h after APAP exposure. The increased hepatic transcription of Il-6 coincided with higher levels of circulating Il-6. Consistent with greater Il-6 expression, APAP-exposed AKBI mice demonstrated increased hepatic STAT3 activation. Prior work interrogating the role of Il-6/STAT3 activation after APAP is nuanced. Il-6 knock-out mice demonstrate decreased STAT3 activation, worse injury, and impaired hepatic regeneration after APAP, indicating that some Il-6/STAT3 signaling is necessary for liver repair (James *et al.*, 2003). However, our results add to the growing body of evidence demonstrating that exaggerated Il-6/STAT3 activation is associated with worse hepatic injury and outcomes after APAP overdose. Several prior studies demonstrate that increased Il-6 induction and hepatic STAT3 activation correlate with greater hepatotoxicity after APAP exposure (Bhushan *et al.*, 2014; Numata *et al.*, 2007). It has been reported that therapeutic strategies that improve hepatic injury after APAP also result in decreased Il-6 production (Guo *et al.*, 2019; Lee *et al.*, 2019; Shi *et al.*, 2012; Zhan *et al.*, 2020). Additionally, administration of an Il-6 neutralizing antibody attenuated APAP-induced hepatic injury in genetically modified mice that demonstrate an exaggerated Il-6 response (Bourdi *et al.*, 2007). Finally, other models such as partial hepatectomy demonstrate that overactive Il-6/STAT3 is associated with impaired liver generation and histopathologic damage (Torbenson *et al.*, 2002; Wüstefeld *et al.*, 2000). Importantly, increased hepatic Il-6 and STAT3 have been observed in mice with sinusoidal dilation after drug exposure to chemotherapeutic agents including 5-fluorouracil and oxaliplatin (Robinson *et al.*, 2013). The AKBI mice also demonstrated increased sinusoidal dilation compared with

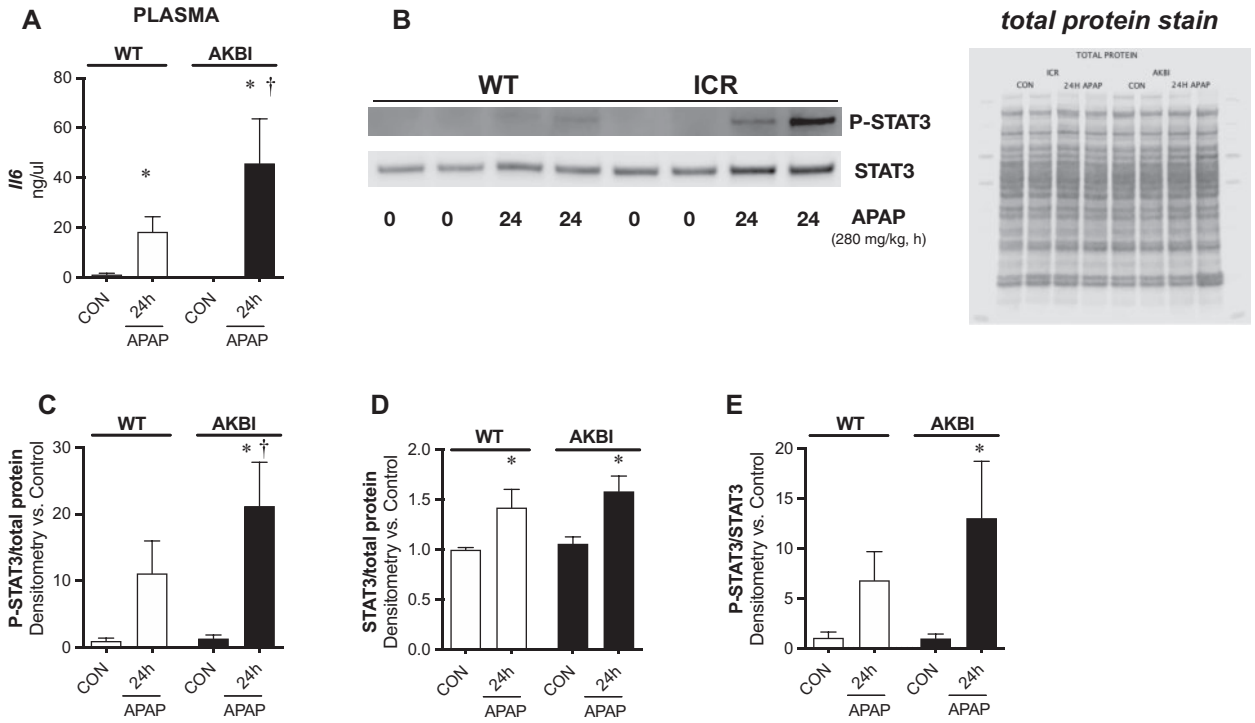

Figure 7. Toxic acetaminophen (APAP) exposure induces exaggerated hepatic signal transducer and activator of transcription 3 (STAT3) activation in AKBI mice. Wild type (WT) and AKBI (IkappaB beta knock-in mice) were exposed to APAP (280 mg/kg, IP) for 0 or 24 h. A, Total serum Il-6 protein. B, Representative Western blot of phosphorylated STAT3 (pSTAT3) and STAT3 in whole liver homogenates, with total protein shown as loading control. Densitometric analysis of C, pSTAT3, D, Total STAT3, and E, pSTAT3/Total STAT3 ratio. White columns represent WT mice and black columns represent AKBI mice ($n = 4$–9). Data are expressed as mean ± SEM; $^{*}p < .05$ versus genotype-matched control and $\dagger p < .05$ versus time-matched exposure.

WT mice, supporting a relationship between exaggerated Il-6/STAT3 and sinusoidal dilation after APAP. Further work will need to dissect the temporal and dose-specific relationships to identify what degree of Il-6/STAT3 activation is necessary for liver generation, and if there are therapeutic windows where anti-Il-6 therapy may improve outcomes.

The role of Il-6 in APAP-induced damage in our study and other preclinical reports is consistent with clinical data from patients with APAP overdose. Data from the Acute Liver Failure Study Group demonstrated that Il-6 increases after APAP and that higher plasma Il-6 levels after APAP overdose are observed in patients with worse Model for End Liver Disease (MELD) scores (≥20; Bonkovsky *et al.*, 2018; James *et al.*, 2005; Li *et al.*, 2010). Notably, the clinical reports also indicate that the NFκB and STAT3-dependent cytokine monocyte chemoattractant protein-1 (MCP-1) increases significantly after APAP overdose and is associated with higher transaminitis, longer prothrombin time, and worse MELD scores. This is consistent with our results demonstrating an increase in hepatic *Ccl2*, the gene for MCP-1, in AKBI mice, and supports our observation that an overactive NFκB-associated inflammatory response may be associated with greater injury (Bonkovsky *et al.*, 2018; James *et al.*, 2005).

There are several limitations for this study. Further work is necessary to determine the cell type-specific role of the IκB isoforms in determining the degree and duration of the NFκB response, and this article evaluates the whole liver response without delving into which cell type is responsible. Here, we only evaluated male mice. As it has been established that female mice have decreased susceptibility to APAP exposure, we used male mice to model the most extensive injury in WT mice allowing us to evaluate whether injury would be exacerbated in AKBI mice (Du *et al.*, 2014). Additionally, we did not confirm APAP exposure was similar between genotypes by measuring plasma levels of APAP, although we did use a consistent technique for preparing and administering the APAP. As the AKBI mice demonstrate a robust PSTAT3/STAT3 response, one could speculate that their hepatic regeneration response is intact, and that they would recover at later time points. However, we did not observe later points to determine the role of the IκB isoforms in recovery from injury. Evaluating later time points in conjunction with evaluating apoptosis and markers of cellular regeneration would strengthen our current observations. With this in mind, we only evaluated a toxic dose of APAP in which liver regeneration occurs, and our observations could be strengthened if repeated at a range of doses to determine if IκBβ/NFκB signaling enhances susceptibility to injury at lower doses.

In conclusion, we demonstrate that sustained APAP-induced hepatic NFκB activation in IκBβ knock-in mice is associated with serologic evidence of increased hepatic injury and increased histologic injury including sinusoidal dilatation. The greater degree of liver injury occurred in conjunction with an exaggerated hepatic proinflammatory response, as well as increased Il-6 expression and STAT3 activation. Collectively, these data indicate that targeting sustained NFκB activation mediated by IκBβ may attenuate hepatic injury at later time points following toxic APAP exposure.

AUTHOR CONTRIBUTIONS

L.G.S. and C.J.W. conception and design of research; L.G.S., D.B., L.Z., M.G., W.C.M., R.C.D., D.J.O., and R.D. performed

experiments; L.G.S., D.B., M.G., W.C.M., R.C.D., M.A.Z., R.D., and C.J.W. analyzed data; L.G.S. and C.J.W. interpreted results of experiments; L.G.S. and C.J.W. drafted the article; L.G.S. and C.J.W. prepared figures; L.G.S., M.G., W.C.M., R.C.D., M.A.Z., D.J.O., R.D., and C.J.W. edited and revised article; L.G.S., D.B., L.Z., M.G., W.C.M., R.C.D., M.A.Z., D.J.O., R.D., and C.J.W. approved final version of article.

DATA AVAILABILITY STATEMENT

The data used to support the findings of this study are included within the article.

FUNDING

The National Institutes of Health grant (R01HL132941) to C.J.W. and K12 Child Health Research grant from the University of Colorado Department of Pediatrics to L.G.S.

DECLARATION OF CONFLICTING INTERESTS

The authors declared no potential conflicts of interest with respect to the research, authorship, and/or publication of this article.

REFERENCES

Bernal, W., Lee, W. M., Wendon, J., Larsen, F. S., and Williams, R. (2015). Acute liver failure: A curable disease by 2024? *J. Hepatol*. **62**, S112–S120.

Bernal, W., and Wendon, J. (2013). Acute liver failure. *N. Engl. J. Med*. **369**, 2525–2534.

Bhushan, B., Walesky, C., Manley, M., Gallagher, T., Borude, P., Edwards, G., Monga, S. P., and Apte, U. (2014). Pro-regenerative signaling after acetaminophen-induced acute liver injury in mice identified using a novel incremental dose model. *Am. J. Pathol*. **184**, 3013–3025.

Bonkovsky, H. L., Barnhart, H. X., Foureau, D. M., Steuerwald, N., Lee, W. M., Gu, J., Fontana, R. J., Hayashi, P. J., Chalasani, N., Navarro, V. M., *et al*.; for the US Drug-Induced Liver Injury Network and the Acute Liver Failure Study Group. (2018). Cytokine profiles in acute liver injury-results from the US drug-induced liver injury network (DILIN) and the acute liver failure study group. *PLoS One* **13**, e0206389.

Botta, D., White, C. C., Vliet-Gregg, P., Mohar, I., Shi, S., McGrath, M. B., McConnachie, L. A., and Kavanagh, T. J. (2008). Modulating GSH synthesis using glutamate cysteine ligase transgenic and gene-targeted mice. *Drug Metab. Rev*. **40**, 465–477.

Bourdi, M., Eiras, D. P., Holt, M. P., Webster, M. R., Reilly, T. P., Welch, K. D., and Pohl, L. R. (2007). Role of IL-6 in an IL-10 and IL-4 double knockout mouse model uniquely susceptible to acetaminophen-induced liver injury. *Chem. Res. Toxicol*. **20**, 208–216.

Cheng, J., Ryseck, R., Attar, R., Dambach, D., and Bravo, R. (1998). Functional redundancy of the nuclear factor kappa B inhibitors I kappa B alpha and I kappa B beta. *J. Exp. Med*. **188**, 1055–1062.

Chowdhury, A., Nabila, J., Adelusi Temitope, I., and Wang, S. (2020). Current etiological comprehension and therapeutic targets of acetaminophen-induced hepatotoxicity. *Pharmacol. Res*. **161**, 105102.

Ding, Y., Li, Q., Xu, Y., Chen, Y., Deng, Y., Zhi, F., and Qian, K. (2016). Attenuating oxidative stress by paeonol protected against acetaminophen-induced hepatotoxicity in mice. *PLoS One* **11**, e0154375.

Du, K., Williams, C. D., McGill, M. R., and Jaeschke, H. (2014). Lower susceptibility of female mice to acetaminophen hepatotoxicity: Role of mitochondrial glutathione, oxidant stress and c-jun N-terminal kinase. *Toxicol. Appl. Pharmacol*. **281**, 58–66.

Fan, C., Li, Q., Zhang, Y., Liu, X., Luo, M., Abbott, D., Zhou, W., and Engelhardt, J. F. (2004). IkappaBalpha and ikappaBbeta possess injury context-specific functions that uniquely influence hepatic NF-kappaB induction and inflammation. *J. Clin. Invest*. **113**, 746–755.

Guo, H., Sun, J., Li, D., Hu, Y., Yu, X., Hua, H., Jing, X., Chen, F., Jia, Z., and Xu, J. (2019). Shikonin attenuates acetaminophen-induced acute liver injury via inhibition of oxidative stress and inflammation. *Biomed. Pharmacother*. **112**, 108704.

Hayden, M. S., and Ghosh, S. (2008). Shared principles in NF-kappaB signaling. *Cell* **132**, 344–362.

Horng, C. T., Liu, Z. H., Huang, Y. T., Lee, H. J., and Wang, C. J. (2017). Extract from mulberry (*Morus australis*) leaf decelerate acetaminophen induced hepatic inflammation involving downregulation of myeloid differentiation factor 88 (MyD88) signals. *J. Food Drug Anal*. **25**, 862–871.

Huang, T. T., Kudo, N., Yoshida, M., and Miyamoto, S. (2000). A nuclear export signal in the N-terminal regulatory domain of ikappabalpha controls cytoplasmic localization of inactive NF-kappaB/ikappaBalpha complexes. *Proc. Natl. Acad. Sci. U.S.A*. **97**, 1014–1019.

James, L. P., Lamps, L. W., McCullough, S., and Hinson, J. A. (2003). Interleukin 6 and hepatocyte regeneration in acetaminophen toxicity in the mouse. *Biochem. Biophys. Res. Commun*. **309**, 857–863.

James, L. P., Simpson, P. M., Farrar, H. C., Kearns, G. L., Wasserman, G. S., Blumer, J. L., Reed, M. D., Sullivan, J. E., and Hinson, J. A. (2005). Cytokines and toxicity in acetaminophen overdose. *J. Clin. Pharmacol*. **45**, 1165–1171.

Jan, Y. H., Heck, D. E., Dragomir, A. C., Gardner, C. R., Laskin, D. L., and Laskin, J. D. (2014). Acetaminophen reactive intermediates target hepatic thioredoxin reductase. *Chem. Res. Toxicol*. **27**, 882–894.

Jiang, L., Ke, M., Yue, S., Xiao, W., Yan, Y., Deng, X., Ying, Q. L., Li, J., and Ke, B. (2017). Blockade of notch signaling promotes acetaminophen-induced liver injury. *Immunol. Res*. **65**, 739–749.

Ko, J. W., Park, S. H., Shin, N. R., Shin, J. Y., Kim, J. W., Shin, I. S., Moon, C., Heo, J. D., Kim, J. C., and Lee, I. C. (2017). Protective effect and mechanism of action of diallyl disulfide against acetaminophen-induced acute hepatotoxicity. *Food Chem. Toxicol*. **109**, 28–37.

Lee, H. C., Yu, H. P., Liao, C. C., Chou, A. H., and Liu, F. C. (2019). Escin protects against acetaminophen-induced liver injury in mice via attenuating inflammatory response and inhibiting ERK signaling pathway. *Am. J. Transl. Res*. **11**, 5170–5182.

Li, J., Zhu, X., Liu, F., Cai, P., Sanders, C., Lee, W. M., and Uetrecht, J. (2010). Cytokine and autoantibody patterns in acute liver failure. *J. Immunotoxicol*. **7**, 157–164.

Long, X., Song, J., Zhao, X., Zhang, Y., Wang, H., Liu, X., and Suo, H. (2020). Silkworm pupa oil attenuates acetaminophen-induced acute liver injury by inhibiting oxidative stress-mediated NF-κB signaling. *Food Sci. Nutr*. **8**, 237–245.

Lores Arnaiz, S., Llesuy, S., Cutrin, J. C., and Boveris, A. (1995). Oxidative stress by acute acetaminophen administration in mouse liver. *Free Radic. Biol. Med*. **19**, 303–310.

Martin-Murphy, B. V., Kominsky, D. J., Orlicky, D. J., Donohue, T. M., Jr, and Ju, C. (2013). Increased susceptibility of natural killer T-cell-deficient mice to acetaminophen-induced liver injury. *Hepatology* **57**, 1575–1584.

Marzano, C., Cazals-Hatem, D., Rautou, P. E., and Valla, D. C. (2015). The significance of nonobstructive sinusoidal dilatation of the liver: Impaired portal perfusion or inflammatory reaction syndrome. *Hepatology* **62**, 956–963.

McConnachie, L. A., Mohar, I., Hudson, F. N., Ware, C. B., Ladiges, W. C., Fernandez, C., Chatterton-Kirchmeier, S., White, C. C., Pierce, R. H., and Kavanagh, T. J. (2007). Glutamate cysteine ligase modifier subunit deficiency and gender as determinants of acetaminophen-induced hepatotoxicity in mice. *Toxicol. Sci.* **99**, 628–636.

McKenna, S., Gossling, M., Bugarini, A., Hill, E., Anderson, A. L., Rancourt, R. C., Balasubramaniyan, N., El Kasmi, K. C., and Wright, C. J. (2015). Endotoxemia induces IκBβ/NF-κB-dependent endothelin-1 expression in hepatic macrophages. *J. Immunol.* **195**, 3866–3879.

McKenna, S., Michaelis, K. A., Agboke, F., Liu, T., Han, K., Yang, G., Dennery, P. A., and Wright, C. J. (2014). Sustained hyperoxia-induced NF-κB activation improves survival and preserves lung development in neonatal mice. *Am. J. Physiol. Lung Cell Mol. Physiol.* **306**, L1078–1089.

Michaelis, K. A., Agboke, F., Liu, T., Han, K., Muthu, M., Galambos, C., Yang, G., Dennery, P. A., and Wright, C. J. (2014). IκBβ-mediated nf-κb activation confers protection against hyperoxic lung injury. *Am. J. Respir. Cell Mol. Biol.* **50**, 429–438.

Morgan, M. J., and Liu, Z. G. (2011). Crosstalk of reactive oxygen species and NF-κB signaling. *Cell Res.* **21**, 103–115.

Nathan, C., and Cunningham-Bussel, A. (2013). Beyond oxidative stress: An immunologist's guide to reactive oxygen species. *Nat. Rev. Immunol.* **13**, 349–361.

Numata, K., Kubo, M., Watanabe, H., Takagi, K., Mizuta, H., Okada, S., Kunkel, S. L., Ito, T., and Matsukawa, A. (2007). Overexpression of suppressor of cytokine signaling-3 in T cells exacerbates acetaminophen-induced hepatotoxicity. *J. Immunol.* **178**, 3777–3785.

Pu, S., Liu, Q., Li, Y., Li, R., Wu, T., Zhang, Z., Huang, C., Yang, X., and He, J. (2019). Montelukast prevents mice against acetaminophen-induced liver injury. *Front. Pharmacol.* **10**, 1070.

Rao, P., Hayden, M. S., Long, M., Scott, M. L., West, A. P., Zhang, D., Oeckinghaus, A., Lynch, C., Hoffmann, A., Baltimore, D., *et al.*, (2010). Ikappabbeta acts to inhibit and activate gene expression during the inflammatory response. *Nature* **466**, 1115–1119.

Robinson, S. M., Mann, J., Vasilaki, A., Mathers, J., Burt, A. D., Oakley, F., White, S. A., and Mann, D. A. (2013). Pathogenesis of folfox induced sinusoidal obstruction syndrome in a murine chemotherapy model. *J. Hepatol.* **59**, 318–326.

Sandoval, J., Orlicky, D. J., Allawzi, A., Butler, B., Ju, C., Phan, C. T., Toston, R., De Dios, R., Nguyen, L., McKenna, S., *et al.*, (2019). Toxic acetaminophen exposure induces distal lung ER stress, proinflammatory signaling, and emphysematous changes in the adult murine lung. *Oxid. Med. Cell Longev.* **2019**, 7595126.

Scheibel, M., Klein, B., Merkle, H., Schulz, M., Fritsch, R., Greten, F. R., Arkan, M. C., Schneider, G., and Schmid, R. M. (2010). IkappaBbeta is an essential co-activator for LPS-induced IL-1beta transcription in vivo. *J. Exp. Med.* **207**, 2621–2630.

Sherlock, L. G., Sjostrom, K., Sian, L., Delaney, C., Tipple, T. E., Krebs, N. F., Nozik-Grayck, E., and Wright, C. J. (2020). Hepatic-specific decrease in the expression of selenoenzymes and factors essential for selenium processing after endotoxemia. *Front. Immunol.* **11**, 595282.

Shi, Y., Zhang, L., Jiang, R., Chen, W., Zheng, W., Chen, L., Tang, L., Li, L., Tang, W., Wang, Y., *et al.*, (2012). Protective effects of nicotinamide against acetaminophen-induced acute liver injury. *Int. Immunopharmacol.* **14**, 530–537.

Taniguchi, K., and Karin, M. (2018). NF-κB, inflammation, immunity and cancer: Coming of age. *Nat. Rev. Immunol.* **18**, 309–324.

Torbenson, M., Yang, S. Q., Liu, H. Z., Huang, J., Gage, W., and Diehl, A. M. (2002). STAT-3 overexpression and p21 upregulation accompany impaired regeneration of fatty livers. *Am. J. Pathol.* **161**, 155–161.

Wüstefeld, T., Rakemann, T., Kubicka, S., Manns, M. P., and Trautwein, C. (2000). Hyperstimulation with interleukin 6 inhibits cell cycle progression after hepatectomy in mice. *Hepatology* **32**, 514–522.

Xu, S., Zhi, H., Hou, X., Cohen, R. A., and Jiang, B. (2011). IκBβ attenuates angiotensin II-induced cardiovascular inflammation and fibrosis in mice. *Hypertension* **58**, 310–316.

Yan, M., Huo, Y., Yin, S., and Hu, H. (2018). Mechanisms of acetaminophen-induced liver injury and its implications for therapeutic interventions. *Redox. Biol.* **17**, 274–283.

Yang, R., Zhang, S., Cotoia, A., Oksala, N., Zhu, S., and Tenhunen, J. (2012). High mobility group B1 impairs hepatocyte regeneration in acetaminophen hepatotoxicity. *BMC Gastroenterol.* **12**, 45.

Yang, R., Zhang, S., Kajander, H., Zhu, S., Koskinen, M. L., and Tenhunen, J. (2011). Ringer's lactate improves liver recovery in a murine model of acetaminophen toxicity. *BMC Gastroenterol.* **11**, 125.

Yoon, E., Babar, A., Choudhary, M., Kutner, M., and Pyrsopoulos, N. (2016). Acetaminophen-induced hepatotoxicity: A comprehensive update. *J. Clin. Transl. Hepatol.* **4**, 131–142.

Yuan, K., Zhang, X., Lv, L., Zhang, J., Liang, W., and Wang, P. (2016). Fine-tuning the expression of microRNA-155 controls acetaminophen-induced liver inflammation. *Int. Immunopharmacol.* **40**, 339–346.

Zhan, X., Zhang, J., Chen, H., Liu, L., Zhou, Y., Zheng, T., Li, S., Zhang, Y., Zheng, B., and Gong, Q. (2020). Capsaicin alleviates acetaminophen-induced acute liver injury in mice. *Clin. Immunol.* **220**, 108578.

Zhang, Q., Lenardo, M. J., and Baltimore, D. (2017). 30 years of NF-κB: A blossoming of relevance to human pathobiology. *Cell* **168**, 37–57.